Chapter 1
Synchronization Phenomena

Here we consider the dynamics of complex systems constituted of interacting local computational units that have their own non-trivial dynamics. An example for a local dynamical system is the time evolution of an infectious disease in a certain city that is weakly influenced by an ongoing outbreak of the same disease in another city; or the case of a neuron in a state where it fires spontaneously under the influence of the afferent axon potentials.

A fundamental question is then whether the time evolutions of these local computational unit will remain dynamically independent of each other or whether, at some point, they will start to change their states all in the same rhythm. This is the notion of "synchronization", which we will study throughout this chapter. Starting with the paradigmal Kuramoto model we will learn that synchronization processes may be driven either by averaging dynamical variables or through causal mutual influences.

1.1 Frequency Locking

In this chapter we will be dealing mostly with autonomous dynamical systems which may synchronize spontaneously. A dynamical system may also be driven by outside influences, being forced to follow the external signal synchronously.

The Driven Harmonic Oscillator As an example we consider the driven harmonic oscillator

$$\ddot{x} + \gamma\,\dot{x} + \omega_0^2\,x = F\left(e^{i\omega t} + c.c.\right), \qquad \gamma > 0 \,. \tag{1.1}$$

In the absence of external driving, $F \equiv 0$, the solution is

$$x(t) \sim e^{\lambda t}, \qquad \lambda_{\pm} = -\frac{\gamma}{2} \pm \sqrt{\frac{\gamma^2}{4} - \omega_0^2}\,, \tag{1.2}$$

which is damped/critical/overdamped for $\gamma < 2\omega_0$, $\gamma = 2\omega_0$ and $\gamma > 2\omega_0$.

Frequency Locking In the long time limit, $t \to \infty$, the dynamics of the system follows the external driving, for all $F \neq 0$, due the damping $\gamma > 0$. We therefore consider the ansatz

$$x(t) = ae^{i\omega t} + c.c., \tag{1.3}$$

where the amplitude a may contain an additional time-independent phase. Using this ansatz for Eq. (1.1) we obtain

$$\begin{aligned} F &= a\left(-\omega^2 + i\omega\gamma + \omega_0^2\right) \\ &= -a\left(\omega^2 - i\omega\gamma - \omega_0^2\right) = -a\left(\omega + i\lambda_+\right)\left(\omega + i\lambda_-\right)\ , \end{aligned}$$

where the eigenfrequencies $\lambda_\pm$ are given by Eq. (1.2). The solution for the amplitude a can then be written in terms of $\lambda_\pm$ or alternatively as

$$a = \frac{-F}{(\omega^2 - \omega_0^2) - i\omega\gamma}\ . \tag{1.4}$$

The response becomes divergent, viz $a \to \infty$, at resonance $\omega = \omega_0$ and small damping $\gamma \to 0$.

The General Solution The driven, damped harmonic oscillator Eq. (1.1) is an inhomogeneous linear differential equation and its general solution is given by the superposition of the special solution Eq. (1.4) with the general solution of the homogeneous system Eq. (1.2). The latter dies out for $t \to \infty$ and the system synchronizes with the external driving frequency ω.

1.2 Coupled Oscillators and the Kuramoto Model

Any set of local dynamical systems may synchronize, whenever their dynamical behaviours are similarly and the mutual couplings substantial. We start by discussing the simplest non-trivial set-up, viz harmonically coupled harmonic oscillators.

Limiting Cycles A free rotation

$$x(t) = r\Big(\cos(\omega t + \phi_0), \sin(\omega t + \phi_0)\Big), \qquad \theta(t) = \omega t + \theta_0, \qquad \dot{\theta} = \omega$$

often occurs (in suitable coordinates) as limiting cycles of dynamical systems, see Chap. **??**. One can then use the phase variable $\theta(t)$ for an effective description.

Coupled Dynamical Systems We consider a collection of individual dynamical systems $i = 1, \ldots, N$, which have limiting cycles with natural frequencies ω_i. The coupled system then obeys

$$\dot{\theta}_i = \omega_i + \sum_{j=1}^{N} \Gamma_{ij}(\theta_i, \theta_j), \qquad i = 1, \ldots, N \ , \tag{1.5}$$

where the Γ_{ij} are suitable coupling constants.

The Kuramoto Model A particularly tractable choice for the coupling constants Γ_{ij} has been proposed by Kuramoto:

$$\Gamma_{ij}(\theta_i, \theta_j) = \frac{K}{N} \sin(\theta_j - \theta_i) \ , \tag{1.6}$$

where $K \geq 0$ is the coupling strength and the factor $1/N$ ensures that the model is well behaved in the limit $N \to \infty$.

Two Coupled Oscillators We consider first the case $N = 2$:

$$\dot{\theta}_1 = \omega_1 + \frac{K}{2} \sin(\theta_2 - \theta_1), \qquad \dot{\theta}_2 = \omega_2 + \frac{K}{2} \sin(\theta_1 - \theta_2) \ , \tag{1.7}$$

or

$$\Delta\dot{\theta} = \Delta\omega - K \sin(\Delta\theta), \qquad \Delta\theta = \theta_2 - \theta_1, \qquad \Delta\omega = \omega_2 - \omega_1 \ . \tag{1.8}$$

The system has a fixpoint $\Delta\theta^*$ for which

$$\frac{\mathrm{d}}{\mathrm{d}t}\Delta\theta^* = 0, \qquad \sin(\Delta\theta^*) = \frac{\Delta\omega}{K} \tag{1.9}$$

and therefore

$$\Delta\theta^* \in [-\pi/2, \pi/2], \qquad K > |\Delta\omega| \ . \tag{1.10}$$

This condition is valid for attractive coupling constants $K > 0$. For repulsive $K < 0$ anti-phase states are stabilized. We analyze the stability of the fixpoint using $\Delta\theta = \Delta\theta^* + \delta$ and Eq. (1.8). We obtain

$$\frac{\mathrm{d}}{\mathrm{d}t}\delta = -\left(K \cos\Delta\theta^*\right) \delta, \qquad \delta(t) = \delta_0 \, e^{-K \cos\Delta\theta^* t} \ .$$

The fixpoint is stable since $K > 0$ and $\cos\Delta\theta^* > 0$, due to Eq. (1.10). We therefore have a bifurcation.

– For $K < |\Delta\omega|$ there is no phase coherence between the two oscillators, they are drifting with respect to each other.
– For $K > |\Delta\omega|$ there is phase locking and the two oscillators rotate together with a constant phase difference.

This situation is illustrated in Fig. 1.1.

Natural Frequency Distribution We now consider the case of many coupled oscillators, $N \to \infty$. The individual systems have different individual frequencies ω_i with a probability distribution

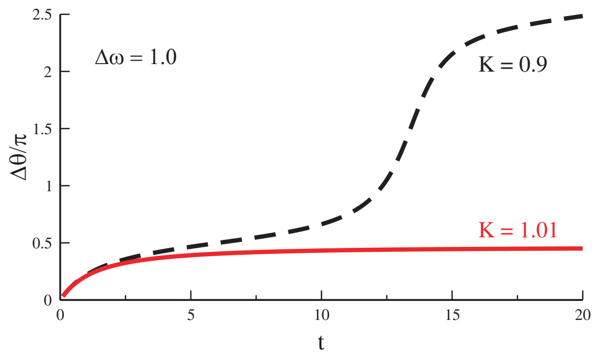

Fig. 1.1 The relative phase $\Delta\theta(t)$ of two coupled oscillators, obeying Eq. (1.8), with $\Delta\omega = 1$ and a critical coupling strength $K_c = 1$. For an undercritical coupling strength $K = 0.9$ the relative phase increases steadily, for an overcritical coupling $K = 1.01$ it locks

$$g(\omega) = g(-\omega), \qquad \int_{-\infty}^{\infty} g(\omega)\,\mathrm{d}\omega = 1 \; . \tag{1.11}$$

We note that the choice of a zero average frequency

$$\int_{-\infty}^{\infty} \omega\, g(\omega)\,\mathrm{d}\omega = 0$$

implicit in Eq. (1.11) is actually generally possible, as the dynamical equations (1.5) and (1.6) are invariant under a global translation

$$\omega \to \omega + \Omega, \qquad \theta_i \to \theta_i + \Omega t \; ,$$

with Ω being the initial non-zero mean frequency.

The Order Parameter The complex order parameter

$$r\, e^{i\psi} = \frac{1}{N} \sum_{j=1}^{N} e^{i\theta_j} \tag{1.12}$$

is a macroscopic quantity that can be interpreted as the collective rhythm produced by the assembly of the interacting oscillating systems. The radius $r(t)$ measures the degree of phase coherence and $\psi(t)$ corresponds to the average phase.

Molecular Field Representation We rewrite the order parameter definition Eq. (1.12) as

$$r\, e^{i(\psi - \theta_i)} = \frac{1}{N} \sum_{j=1}^{N} e^{i(\theta_j - \theta_i)}, \qquad r \sin(\psi - \theta_i) = \frac{1}{N} \sum_{j=1}^{N} \sin(\theta_j - \theta_i) \; ,$$

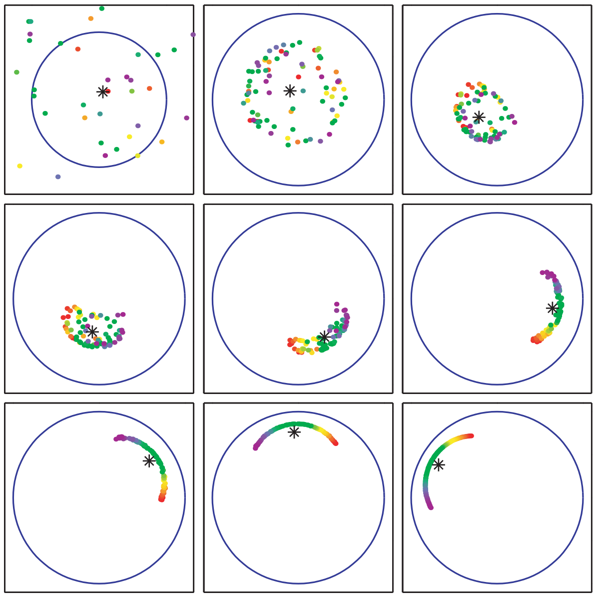

Fig. 1.2 Spontaneous synchronization in a network of limit cycle oscillators with distributed individual frequencies. Color coding: slowest (*red*)–fastest (*violet*) natural frequency. With respect to Eq. (1.5) an additional distribution of individual radii $r_i(t)$ has been assumed, the *asterisk* denotes the mean field $re^{i\psi} = \sum_i r_i e^{i\theta_i}/N$, compare Eq. (1.12), and the individual radii $r_i(t)$ are slowly relaxing (From **? ?**)

retaining the imaginary component of the first term. Inserting the second expression into the governing equation (1.5) we find

$$\dot{\theta}_i = \omega_i + \frac{K}{N}\sum_j \sin(\theta_j - \theta_i) = \omega_i + Kr\sin(\psi - \theta_i) \ . \tag{1.13}$$

The motion of every individual oscillator $i = 1, \dots, N$ is coupled to the other oscillators only through the mean-field phase ψ; the coupling strength being proportional to the mean-field amplitude r.

The individual phases θ_i are drawn towards the self-consistently determined mean phase ψ, as can be seen in the numerical simulations presented in Fig. 1.2. Mean-field theory is exact for the Kuramoto model. It is nevertheless non-trivial to solve, as the self-consistency condition (1.12) needs to be fulfilled.

The Rotating Frame of Reference The order parameter $re^{i\psi}$ performs a free rotation in the thermodynamic limit, and for long times $t \to \infty$,

$$r(t) \to r, \qquad \psi(t) \to \Omega t, \qquad N \to \infty \ ,$$

and one can transform via

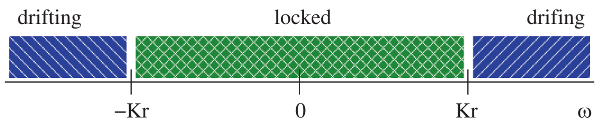

Fig. 1.3 The region of locked and drifting natural frequencies $\omega_i \to \omega$ within the Kuramoto model

$$\theta_i \to \theta_i + \psi = \theta_i + \Omega t, \qquad \dot{\theta}_i \to \theta_i + \Omega, \qquad \omega_i \to \omega_i + \Omega$$

to the rotating frame of reference. The governing equation (1.13) then becomes

$$\dot{\theta}_i = \omega_i - Kr\sin(\theta_i) \ . \tag{1.14}$$

This expression is identical to the one for the case of two coupled oscillators, Eq. (1.8), when substituting Kr by K. It then follows directly that $\omega_i = Kr$ constitutes a special point.

Drifting and Locked Components Equation (1.14) has a fixpoint θ_i^* for which $\dot{\theta}_i^* = 0$ and

$$Kr\sin(\theta_i^*) = \omega_i, \qquad |\omega_i| < Kr, \qquad \theta_i^* \in \left[-\frac{\pi}{2}, \frac{\pi}{2}\right] \ . \tag{1.15}$$

$\dot{\theta}_i^* = 0$ in the rotating frame of reference means that the participating limit cycles oscillate with the average frequency ψ; they are "locked" to ψ, see Figs. 1.2 and 1.3.

For $|\omega_i| > Kr$ the participating limit cycle *drifts*, i.e. $\dot{\theta}_i$ never vanishes. They do, however, slow down when they approach the locked oscillators, see Eq. (1.14) and Fig. 1.1.

Stationary Frequency Distribution We denote by

$$\rho(\theta, \omega)\,\mathrm{d}\theta$$

the fraction of evolving oscillators with natural frequency ω that lie between θ and $\theta + \mathrm{d}\theta$. It obeys the continuity equation

$$\frac{\partial \rho}{\partial t} + \frac{\partial}{\partial \theta}\left(\rho\,\dot{\theta}\right) = 0 \ ,$$

where $\rho\dot{\theta}$ is the respective current density. In the stationary case, $\dot{\rho} = 0$, the stationary frequency distribution $\rho(\theta, \omega)$ needs to be inversely proportional to the speed

$$\dot{\theta} = \omega - Kr\sin(\theta) \ .$$

The oscillators pile up at slow places and thin out at fast places on the circle. Hence

$$\rho(\theta,\omega) = \frac{C}{|\omega - Kr\sin(\theta)|}, \qquad \int_{-\pi}^{\pi} \rho(\theta,\omega)\,\mathrm{d}\theta = 1 \ , \tag{1.16}$$

for $\omega > 0$, where C is an appropriate normalization constant.

Formulation of the Self-consistency Condition We write the self-consistency condition (1.12) as

$$\langle e^{i\theta}\rangle = \langle e^{i\theta}\rangle_{\mathrm{locked}} + \langle e^{i\theta}\rangle_{\mathrm{drifting}} = r\,e^{i\psi} \equiv r \ , \tag{1.17}$$

where the brackets $\langle\cdot\rangle$ denote population averages and where we have used the fact that we can set the average phase ψ to zero.

Locked Contribution The locked contribution is

$$\langle e^{i\theta}\rangle_{\mathrm{locked}} = \int_{-Kr}^{Kr} e^{i\theta^*(\omega)} g(\omega)\,\mathrm{d}\omega = \int_{-Kr}^{Kr} \cos\left((\theta^*(\omega)\right)\, g(\omega)\,\mathrm{d}\omega \ ,$$

where we have assumed $g(\omega) = g(-\omega)$ for the distribution $g(\omega)$ of the natural frequencies within the rotating frame of reference. Using Eq. (1.15),

$$\mathrm{d}\omega = Kr\cos\theta^*\,\mathrm{d}\theta^* \ ,$$

for $\theta^*(\omega)$ we obtain

$$\begin{aligned} \langle e^{i\theta}\rangle_{\mathrm{locked}} &= \int_{-\pi/2}^{\pi/2} \cos(\theta^*)\, g(Kr\sin\theta^*)\, Kr\ \cos(\theta^*)\,\mathrm{d}\theta^* \qquad (1.18)\\ &= Kr\int_{-\pi/2}^{\pi/2} \cos^2(\theta^*)\, g(Kr\sin\theta^*)\,\mathrm{d}\theta^* \ . \end{aligned}$$

The Drifting Contribution The drifting contribution

$$\langle e^{i\theta}\rangle_{\mathrm{drifting}} = \int_{-\pi}^{\pi} \mathrm{d}\theta \int_{|\omega|>Kr} \mathrm{d}\omega\, e^{i\theta}\rho(\theta,\omega)g(\omega) = 0$$

to the order parameter actually vanishes. Physically this is clear: oscillators that are not locked to the mean field cannot contribute to the order parameter. Mathematically it follows from $g(\omega) = g(-\omega)$, $\rho(\theta+\pi,-\omega) = \rho(\theta,\omega)$ and $e^{i(\theta+\pi)} = -e^{i\theta}$.

Second-Order Phase Transition The population average $\langle e^{i\theta}\rangle$ of the order parameter Eq. (1.17) is then just the locked contribution Eq. (1.18)

$$r = \langle e^{i\theta}\rangle \equiv \langle e^{i\theta}\rangle_{\mathrm{locked}} = Kr\int_{-\pi/2}^{\pi/2} \cos^2(\theta^*)\, g(Kr\sin\theta^*)\,\mathrm{d}\theta^* \ . \tag{1.19}$$

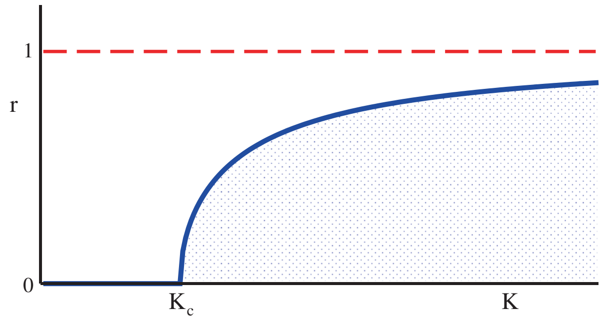

Fig. 1.4 The solution $r=\sqrt{1-K_c/K}$ for the order parameter r in the Kuramoto model, compare Eq. (1.21)

For $K < K_c$ Eq. (1.19) has only the trivial solution $r = 0$; for $K > K_c$ a finite order parameter $r > 0$ is stabilized, see Fig. 1.4. We therefore have a second-order phase transition, as discussed in Chap. **??**.

Critical Coupling The critical coupling strength K_c can be obtained considering the limes $r \to 0+$ in Eq. (1.19):

$$1 = K_c\, g(0) \int_{-\pi/2}^{\pi/2} \cos^2\theta^*\, \mathrm{d}\theta^* = K_c\, g(0) \frac{\pi}{2}, \qquad K_c = \frac{2}{\pi g(0)}\ . \tag{1.20}$$

The self-consistency condition Eq. (1.19) can actually be solved exactly with the result

$$r = \sqrt{1-\frac{K_c}{K}}, \qquad K_c = \frac{2}{\pi g(0)}\ , \tag{1.21}$$

as illustrated in Fig. 1.4.

The Physics of Rhythmic Applause A nice application of the Kuramoto model is the synchronization of the clapping of an audience after a performance, which happens when everybody claps at a slow frequency and in tact. In this case the distribution of "natural clapping frequencies" is quite narrow and $K > K_c \propto 1/g(0)$.

When an individual wants to express especial satisfaction with the performance he/she increases the clapping frequency by about a factor of 2, as measured experimentally, in order to increase the noise level, which just depends on the clapping frequency. Measurements have shown, see Fig. 1.5, that the distribution of natural clapping frequencies is broader when the clapping is fast. This leads to a drop in $g(0)$ and then $K < K_c \propto 1/g(0)$. No synchronization is possible when the applause is intense.

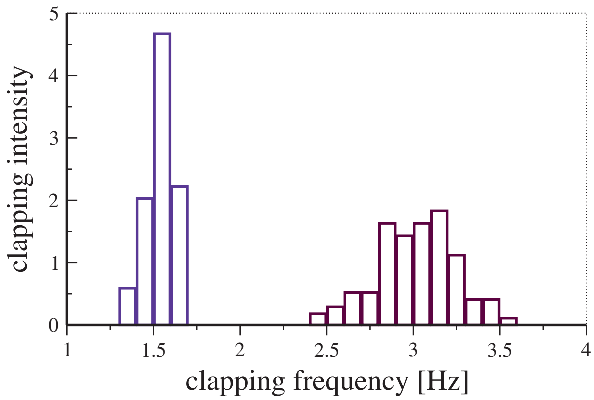

Fig. 1.5 Normalized distribution for the frequencies of clappings of one chosen individual from 100 samplings (**??**)

1.3 Synchronization in the Presence of Time Delays

Synchronization phenomena need the exchange of signals from one subsystem to another and this information exchange typically needs a certain time. These time delays become important when they are comparable to the intrinsic time scales of the individual subsystems. A short introduction into the intricacies of time-delayed dynamical systems has been given in Sect. **??**, here we discuss the effect of time delays on the synchronization process.

The Kuramoto Model with Time Delays We start with two limiting-cycle oscillators, coupled via a time delay T:

$$\dot{\theta}_1(t) = \omega_1 + \frac{K}{2}\,\sin[\theta_2(t-T)-\theta_1(t)], \qquad \dot{\theta}_2(t) = \omega_2 + \frac{K}{2}\,\sin[\theta_1(t-T)-\theta_2(t)]\ .$$

In the steady state,

$$\theta_1(t) = \omega\, t, \qquad\qquad \theta_2(t) = \omega\, t + \Delta\theta^*\ , \tag{1.22}$$

there is a synchronous oscillation with a yet to be determined locking frequency ω and a phase slip $\Delta\theta^*$. Using $\sin(\alpha+\beta) = \sin(\alpha)\cos(\beta) + \cos(\alpha)\sin(\beta)$ we find

$$\begin{aligned} \omega &= \omega_1 + \frac{K}{2}\big[-\sin(\omega T)\cos(\Delta\theta^*) + \cos(\omega T)\sin(\Delta\theta^*)\big], \\ \omega &= \omega_2 + \frac{K}{2}\big[-\sin(\omega T)\cos(\Delta\theta^*) - \cos(\omega T)\sin(\Delta\theta^*)\big]\ . \end{aligned} \tag{1.23}$$

Taking the difference we obtain

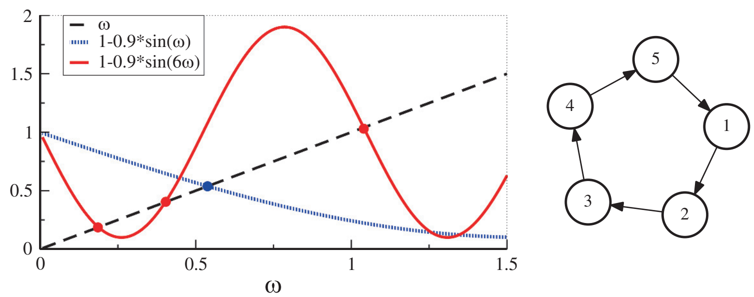

Fig. 1.6 *Left*: Graphical solution of the self-consistency condition (1.25), given by the intersections of the *dashed* with the *solid* and *shaded* lines, for the locking frequency ω, and time delays $T = 1$ (one solution) and $T = 6$ (three solutions in the interval $\omega \in [0, 1.5]$). The coupling constant is $K = 1.8$. *Right*: An example of a directed ring, containing five sites

$$\Delta\omega = \omega_2 - \omega_1 = K \sin(\Delta\theta^*) \cos(\omega T) \ , \tag{1.24}$$

which generalizes Eq. (1.9) to the case of a finite time delay T. Equations (1.23) and (1.24) then determine together locking frequency ω and the phase slip $\Delta\theta^*$.

Multiple Synchronization Frequencies For finite time delays T, there are generally more than one solution for the synchronization frequency ω. For concreteness we consider now the case

$$\omega_1 = \omega_2 \equiv 1, \qquad \Delta\theta^* \equiv 0, \qquad \omega = 1 - \frac{K}{2}\sin(\omega T) \ , \tag{1.25}$$

compare Eqs. (1.24) and (1.23). This equation can be solved graphically, see Fig. 1.6.

For $T \to 0$ the two oscillators are phase locked, oscillating with the original natural frequency $\omega = 1$. A finite time delay then leads to a change of the synchronization frequency and eventually, for large enough time delay T and couplings K, to multiple solutions for the locking frequency. These solutions are stable for

$$K \cos(\omega T) > 0 \ ; \tag{1.26}$$

we leave the derivation as an exercise to the reader. The time delay such results in a qualitative change in the structure of the phase space.

Rings of Delayed-Coupled Oscillators As an example of the possible complexity arising from delayed couplings we consider a ring of N oscillators, as illustrated in Fig. 1.6, coupled unidirectionally,

$$\dot{\theta}_j = \omega_j + K \sin[\theta_{j-1}(t - T) - \theta_j(t)], \qquad j = 1, \ldots, N \ . \tag{1.27}$$

The periodic boundary conditions imply that $N+1\hat{=}1$ in Eq. (1.27). We specialize to the uniform case $\omega_j \equiv 1$. The network is then invariant under rotations of multiples of $2\pi/N$.

We consider plane-wave solutions[1] with frequency ω and momentum k,

$$\theta_j = \omega\, t - k\, j, \qquad k = n_k \frac{2\pi}{N}, \qquad n_k = 0, \dots, N-1 \ , \tag{1.28}$$

where $j = 1, \dots, N$. For $N = 2$ only in-phase $k = 0$ and anti-phase $k = \pi$ solutions exist. The locking frequency ω is then determined by the self-consistency condition

$$\omega = 1 + K \sin(k - \omega T) \ . \tag{1.29}$$

For a given momentum k a set of solutions is obtained. The resulting solutions $\theta_j(t)$ are characterized by complex spatio-temporal symmetries, oscillating fully in phase only for vanishing momentum $k \to 0$. Note however, that additional unlocked solutions cannot be excluded and may show up in numerical solutions. It is important to remember in this context, as discussed in Sect. **??**, that initial conditions in the entire interval $t \in [-T, 0]$ need to be provided.

1.4 Synchronization Mechanisms

The synchronization of the limiting cycle oscillators discussed in Sect. 1.2 is mediated by a molecular field, which is an averaged quantity. Averaging plays a central role in many synchronization processes and may act both on a local basis and on a global level. Alternatively, synchronization may be driven by the casual influence of temporally well defined events, a route to synchronization we will discuss in Sect. 1.4.2.

1.4.1 Aggregate Averaging

The coupling term of the Kuramoto model, see Eq. (1.6), contains differences $\theta_i - \theta_j$ in the respective dynamical variables θ_i and θ_j. With an appropriate sign of the coupling constant, this coupling results in a driving force towards the average,

$$\theta_1 \to \frac{\theta_1 + \theta_2}{2}, \qquad \theta_2 \to \frac{\theta_1 + \theta_2}{2} \ .$$

[1] In the complex plane $\psi_j(t) = e^{i\theta_j(t)} = e^{i(\omega t - kj)}$ corresponds to a plane wave on a periodic ring. Equation (1.27) is then equivalent to the phase evolution of the wavefunction $\psi_j(t)$. The system is invariant under translations $j \to j+1$ and the discrete momentum k is therefore a good quantum number, in the jargon of quantum mechanics. The periodic boundary condition $\psi_{j+N} = \psi_j$ is satisfied for the momenta $k = 2\pi n_k/N$.

This driving force competes with the differences in the time-development of the individual oscillators, which is present whenever their natural frequencies ω_i and ω_j do not coincide. A detailed analysis is then necessary, as carried out in Sect. 1.2, in order to study this competition between the synchronizing effect of the coupling and the desynchronizing influence of a non-trivial natural frequency distribution.

Aggregate Variables Generalizing above considerations we consider now a set of dynamical variables x_i, with $\dot{x}_i = f_i(x_i)$ being the evolution rule for the isolated units. The geometry of the couplings is given by the normalized weighted adjacency matrix

$$A_{ij}, \qquad \sum_j A_{ij} = 1 \ .$$

The matrix elements are $A_{ij} > 0$ if the units i and j are coupled, and zero otherwise, compare Chap. **??**, with A_{ij} representing the relative weight of the link. We define now the aggregate variables $\bar{x}_i = \bar{x}_i(t)$ by

$$\bar{x}_i = (1-\kappa_i)x_i + \kappa_i \sum_j A_{ij} x_j \ , \tag{1.30}$$

where $\kappa_i \in [0,1]$ is the local coupling strength. The aggregate variables $\bar{x}_i$ correspond to a superposition of x_i with the weighted mean activity $\sum_j A_{ij} x_j$ of all its neighbors.

Coupling via Aggregate Averaging A quite general class of dynamical networks can now be formulated in terms of aggregate variables through

$$\dot{x}_i = f_i(\bar{x}_i), \qquad i = 1, \ldots, N \ , \tag{1.31}$$

with the $\bar{x}_i$ given by Eq. (1.30). The f_i describe the local dynamical systems which could be, e.g., harmonic oscillators, relaxation oscillators or chaotic systems.

Expansion around the Synchronized State In order to expand Eq. (1.31) around the globally synchronized state we first rewrite the aggregate variables as

$$\begin{aligned} \bar{x}_i &= (1-\kappa_i)x_i + \kappa_i \sum_j A_{ij}(x_j - x_i + x_i) \qquad (1.32) \\ &= x_i\Big(1 - \kappa_i + \kappa_i \sum_j A_{ij}\Big) + \kappa_i \sum_j A_{ij}(x_j - x_i) = x_i + \kappa_i \sum_j A_{ij}(x_j - x_i) \ , \end{aligned}$$

where we have used the normalization $\sum_j A_{ij} = 1$. The differences in activities $x_j - x_i$ are small close to the synchronized state and we may expand

$$f_i(\bar{x}_i) \approx f_i(x_i) + f_i'(x_i)\kappa_i \sum_j A_{ij}(x_j - x_i) \ . \tag{1.33}$$

Differential couplings $\sim(x_j - x_i)$ between the nodes of the network are hence equivalent, close to synchronization, to the aggregate averaging of the local dynamics via the respective $\bar{x}_i$.

General Coupling Functions We may go one step further and define with

$$\dot{x}_i = f_i(x_i) + h_i(x_i) \sum_j g_{ij}(x_j - x_i) \tag{1.34}$$

a general system of $i = 1, \ldots, N$ dynamical units interacting via the coupling functions $g_{ij}(x_j - x_i)$, which are respectively modulated through the $h_i(x_i)$. Close to the synchronized state we may expand Eq. (1.34) as

$$\dot{x}_i \approx f_i(x_i) + h_i(x_i) \sum_j g_{ij}'(0)(x_j - x_i), \qquad h_i(x_i)g_{ij}'(0) \mathrel{\hat{=}} f_i'(x_i)\kappa_i A_{ij} \ .$$

The equivalence of $h_i(x_i)g_{ij}'(0)$ and $f_i'(x_i)\kappa_i A_{ij}$, compare Eq. (1.33), is local in time, but this equivalence is sufficient for a local stability analysis; the synchronized state of the system with differential couplings, Eq. (1.34), is locally stable whenever the corresponding system with aggregate couplings, Eq. (1.31), is also stable against perturbations.

Synchronization via Aggregated Averaging The equivalence of Eqs. (1.31) and (1.34) tells us that the driving forces leading to synchronization are aggregated averaging processes of neighboring dynamical variables.

Till now we considered globally synchronized states. Synchronization processes are however in general quite intricate processes, we mention here two alternative possibilities. Above discussion concerning aggregate averaging remains however valid, when generalized suitably, also for these more generic synchronized states.

- We saw, when discussing the Kuramoto model in Sect. 1.2, that generically not all nodes of a network participate in a synchronization process. For the Kuramoto model the oscillators with natural frequencies far away from the average do not become locked to the time development of the order parameter, see Fig. 1.3, retaining drifting trajectories.
- Generically, synchronization takes the form of coherent time evolution with phase lags, we have seen an example when discussing two coupled oscillators in Sect. 1.2. The synchronized orbit is then

  $$x_i(t) = x(t) + \Delta x_i, \qquad \Delta x_i \ \text{const.} \ ,$$

  viz the elements $i = 1, \ldots, N$ are all locked in.

Stability Analysis of the Synchronized State The stability of a globally synchronized state, $x_i(t) = x(t)$ for $i = 1, \ldots, N$, can be determined by considering small perturbations, viz

$$x_i(t) = x(t) + \delta_i\, c^t, \qquad |c|^t = e^{\lambda t} \ , \tag{1.35}$$

where λ is the Lyapunov exponent. The eigenvectors $(\delta_1, \ldots, \delta_N)$ of the perturbation are determined by the equations of motion linearized around the synchronized trajectory. There is one Lyapunov exponent for every eigenvector, N in all,

$$\lambda^\alpha, \qquad (\delta_1^\alpha, \ldots, \delta_N^\alpha), \qquad \alpha = 1, \ldots, N \ .$$

One of the exponents, namely

$$\lambda^1 \equiv \lambda^s, \qquad \delta_i^s = \delta, \qquad i = 1, \ldots, N \ ,$$

characterizes the flow along the synchronized direction. The synchronized state is stable if all the remaining λ^j $(j = 2, \ldots, N)$ Lyapunov exponents are negative.

δ^s itself can be either positive or negative. In the case that the synchronized state is periodic, with period T, its integral over one period vanishes,

$$\int_0^T \delta^s(t)\, dt = 0, \tag{1.36}$$

as discussed in Chap. **??**, with expression (1.36) being actually valid for any closed trajectory; the increase (or decrease) of the velocity of the flow would otherwise add at infinitum.

Coupled Logistic Maps As an example we consider two coupled logistic maps, see Fig. **??**,

$$x_i(t+1) = r\, \bar{x}_i(t)\big(1 - \bar{x}_i(t)\big), \qquad i = 1, 2, \qquad r \in [0, 4] \ , \tag{1.37}$$

with

$$\bar{x}_1 = (1-\kappa)x_1 + \kappa x_2, \qquad \bar{x}_2 = (1-\kappa)x_2 + \kappa x_1$$

and $\kappa \in [0, 1]$ being the coupling strength. Using Eq. (1.35) as an Ansatz we obtain

$$c \begin{pmatrix} \delta_1 \\ \delta_2 \end{pmatrix} = r\big(1 - 2x(t)\big) \begin{pmatrix} (1-\kappa) & \kappa \\ \kappa & (1-\kappa) \end{pmatrix} \begin{pmatrix} \delta_1 \\ \delta_2 \end{pmatrix} \ ,$$

which determines c as the eigenvalues of the Jacobian of Eq. (1.37). We have hence two local pairs of eigenvalues and eigenvectors, namely

$$c_1 = r(1-2x) \qquad (\delta_1, \delta_2) = \frac{1}{\sqrt{2}}(1, 1)$$
$$c_2 = r(1-2x)(1-2\kappa) \qquad (\delta_1, \delta_2) = \frac{1}{\sqrt{2}}(1, -1)$$

corresponding to the respective local Lyapunov exponents, $\lambda = \log|c|$,

$$\lambda_1 = \log|r(1-2x)|, \qquad \lambda_2 = \log|r(1-2x)(1-2\kappa)| \,. \tag{1.38}$$

As expected, $\lambda_1 > \lambda_2$, since λ_1 corresponds to a perturbation along the synchronized orbit. The overall stability of the synchronized trajectory can be examined by averaging above local Lyapunov exponents over the full time development, obtaining such the maximal Lyapunov exponent, as defined in Chap. **??**.

Synchronization of Coupled Chaotic Maps The Lyapunov exponents need to be evaluated numerically, but we can obtain an lower bound for the coupling strength κ needed for stable synchronization by observing that $|1-2x| \le 1$ and hence

$$|c_2| \le r|1-2\kappa| \,.$$

The synchronized orbit is stable for $|c_2| < 1$. Considering the case $\kappa \in [0, 1/2]$ we find

$$1 > r(1-2\kappa_s) \ge |c_2|, \qquad \kappa_s > \frac{r-1}{2r}$$

for the lower bound for κ_s. The logistic map is chaotic for $r > r_\infty \approx 3.57$ and above result, being valid for all $r \in [0, 4]$, therefore proves that also chaotic coupled systems may synchronize.

For the maximal reproduction rate, $r = 4$, synchronization is guaranteed for $3/8 < \kappa_s \le 1/2$. Note that $\bar{x}_1 = \bar{x}_2$ for $\kappa = 1/2$, synchronization through aggregate averaging is hence achieved in one step for $\kappa = 1/2$.

1.4.2 Causal Signaling

The synchronization of the limiting cycle oscillators discussed in Sect. 1.2 is very slow, see Fig. 1.2, as the information between the different oscillators is exchanged only indirectly via the molecular field, which is an averaged quantity. Synchronization may be sustantially faster, when the local dynamical units influence each other with precisely timed signals, the route to synchronization discussed here.

Relaxational oscillators, like the van der Pol oscillator discussed in Chap. **??** have a non-uniform cycle and the timing of the stimulation of one element by another is important. This is a characteristic property of real-world neurons in particular and of many models of artificial neurons, like the so-called integrate-and-fire models. Relaxational oscillators are hence well suited to study the phenomena of synchronization via causal signaling.

Terman–Wang Oscillators There are many variants of relaxation oscillators relevant for describing integrate-and-fire neurons, starting from the classical Hodgkin–Huxley equations. Here we discuss the particularly trans-

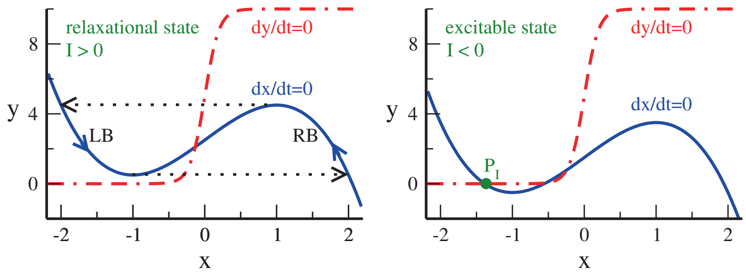

Fig. 1.7 The $\dot{y} = 0$ (*thick dashed-dotted lines*) and the $\dot{x} = 0$ (*thick full lines*) isocline of the Terman–Wang oscillator, Eq. (1.39), for $\alpha = 5$, $\beta = 0.2$, $\epsilon = 0.1$. *Left*: $I = 0.5$ with the limiting relaxational cycle for $\epsilon \ll 1$ (*thin dotted line arrows*). *Right*: $I = -0.5$ with the stable fixpoint: P_I

parent dynamical system introduced by Terman and Wang, namely

$$\begin{array}{ll} \dot{x} = f(x) - y + I & \qquad f(x) = 3x - x^3 + 2 \\ \dot{y} = \epsilon\left(g(x) - y\right) & \qquad g(x) = \alpha\left(1 + \tanh(x/\beta)\right) \end{array} . \tag{1.39}$$

Here x corresponds in neural terms to the membrane potential and I represents the external stimulation to the neural oscillator. The amount of dissipation is given by

$$\frac{\partial \dot{x}}{\partial x} + \frac{\partial \dot{y}}{\partial y} = 3 - 3x^2 - \epsilon = 3(1 - x^2) - \epsilon \ .$$

For small $\epsilon \ll 1$ the system takes up energy for membrane potentials $|x| < 1$ and dissipates energy for $|x| > 1$.

Fixpoints The fixpoints are determined via

$$\begin{array}{ll} \dot{x} = 0 & \qquad y = f(x) + I \\ \dot{y} = 0 & \qquad y = g(x) \end{array}$$

by the intersection of the two functions $f(x) + I$ and $g(x)$, see Fig. 1.7. We find two parameter regimes:

– For $I \geq 0$ we have one unstable fixpoint (x^*, y^*) with $x^* \simeq 0$.
– For $I < 0$ and $|I|$ large enough we have two additional fixpoints given by the crossing of the sigmoid $\alpha\big(1 + \tanh(x/\beta)\big)$ with the left branch (LB) of the cubic $f(x) = 3x - x^3 + 2$, with one fixpoint being stable.

The stable fixpoint P_I is indicated in Fig. 1.7.

The Relaxational Regime For the case $I > 0$ the Terman–Wang oscillator relaxes in the long time limit to a periodic solution, see Fig. 1.7, which is very similar to the limiting relaxation oscillation of the Van der Pol oscillator discussed in Chap. **??**.

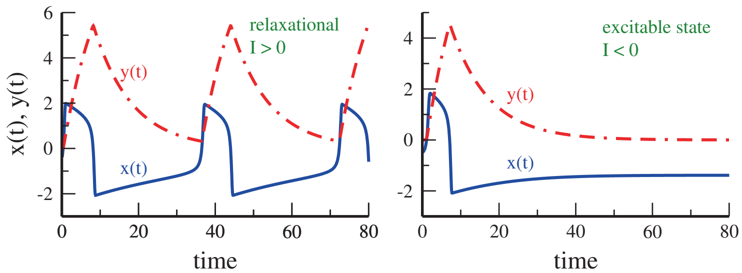

Fig. 1.8 Sample trajectories $y(t)$ (*thick dashed-dotted lines*) and $x(t)$ (*thick full lines*) of the Terman–Wang oscillator Eq. (1.39) for $\alpha = 5$, $\beta = 0.2$, $\epsilon = 0.1$. *Left*: $I = 0.5$ exhibiting spiking behavior, having silent/active phases for negative/positive x. *Right*: $I = -0.5$, relaxing to the stable fixpoint

Silent and Active Phases In its relaxational regime, the periodic solution jumps very fast (for $\epsilon \ll 1$) between trajectories that approach closely the right branch (RB) and the left branch (LB) of the $\dot{x} = 0$ isocline. The time development on the RB and the LB are, however, not symmetric, see Figs. 1.7 and 1.8, and we can distinguish two regimes:

The Silent Phase. We call the relaxational dynamics close to the LB ($x < 0$) of the $\dot{x} = 0$ isocline the silent phase or the refractory period.

The Active Phase. We call the relaxational dynamics close to the RB ($x > 0$) of the $\dot{x} = 0$ isocline the active phase.

The relative rate of the time development $\dot{y}$ in the silent and active phases are determined by the parameter α, compare Eq. (1.39).

The active phase on the RB is far from the $\dot{y} = 0$ isocline for $\alpha \gg 1$, see Fig. 1.7, and the time development $\dot{y}$ is then fast. The silent phase on the LB is, however, always close to the $\dot{y} = 0$ isocline and the system spends considerable time there.

The Spontaneously Spiking State and the Separation of Time Scales In its relaxational phase, the Terman–Wang oscillator can therefore be considered as a spontaneously spiking neuron, see Fig. 1.8, with the spike corresponding to the active phase, which might be quite short compared to the silent phase for $\alpha \gg 1$.

The Terman–Wang differential equations (1.39) are examples of a standard technique within dynamical system theory, the coupling of a slow variable, y, to a fast variable, x, which results in a separation of time scales. When the slow variable $y(t)$ relaxes below a certain threshold, see Fig. 1.8, the fast variable $x(t)$ responds rapidly and resets the slow variable. We will encounter further applications of this procedure in Chap. **??**.

The Excitable State The neuron has an additional phase with a stable fixpoint P_I on the LB (within the silent region), for negative external stimulation (suppression) $I < 0$. The dormant state at the fixpoint P_I is "excitable": A positive external stimulation above a small threshold will force a transition into the active phase, with the neuron spiking continuously.

Synchronization via Fast Threshold Modulation Limit cycle oscillators can synchronize, albeit slowly, via the common molecular field, as discussed in Sect. 1.2. A much faster synchronization can be achieved via *fast threshold synchronization* for a network of interacting relaxation oscillators.

The idea is simple. Relaxational oscillators have distinct states during their cycle; we called them the "silent phase" and the "active phase" for the case of the Terman–Wang oscillator. We then assume that a neural oscillator in its (short) active phase changes the threshold I of the other neural oscillator in Eq. 1.39 as

$$I \to I + \Delta I, \qquad \Delta I > 0 \ ,$$

such that the second neural oscillator changes from an excitable state to the oscillating state. This process is illustrated graphically in Fig. 1.9; it corresponds to a signal send from the first to the second dynamical unit. In neural terms: when the first neuron fires, the second neuron follows suit.

Propagation of Activity We consider a simple model

$$\boxed{1} \;\Rightarrow\; \boxed{2} \;\Rightarrow\; \boxed{3} \;\Rightarrow\; \dots$$

of $i = 1, \dots, N$ coupled oscillators $x_i(t)$, $y_i(t)$, all being initially in the excitable state with $I_i \equiv -0.5$. They are coupled via fast threshold modulation, specifically via

$$\Delta I_i(t) = \Theta(x_{i-1}(t)) \ , \tag{1.40}$$

where $\Theta(x)$ is the Heaviside step function. That is, we define an oscillator i to be in its active phase whenever $x_i > 0$. The resulting dynamics is shown in Fig. 1.10. The chain is driven by setting the first oscillator of the chain into the spiking state for a certain period of time. All other oscillators start to spike consecutively in rapid sequence.

1.5 Synchronization and Object Recognition in Neural Networks

Synchronization phenomena can be observed in many realms of the living world. As an example we discuss here the hypothesis of object definition via synchronous neural firing, a proposal by Singer and von der Malsburg which is at the same time both fascinating and controversial.

Temporal Correlation Theory The neurons in the brain have time-dependent activities and can be described by generalized relaxation oscillators, as outlined in the previous section. The "temporal correlation theory" assumes that not only the average activities of individual neurons (the spik-

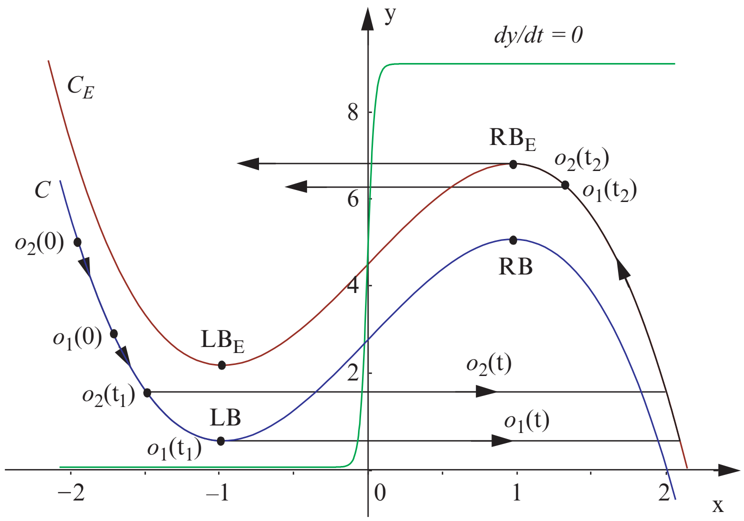

Fig. 1.9 Fast threshold modulation for two excitatory coupled relaxation oscillators, Eq. (1.39) $o_1 = o_1(t)$ and $o_2 = o_2(t)$, which start at time 0. When o_1 jumps at $t = t_1$ the cubic $\dot{x} = 0$ isocline for o_2 is raised from C to C_E. This induces o_2 to jump as well. Note that the jumping from the right branches (RB and RB_E) back to the left branches occurs in the reverse order: o_2 jumps first (From **? ?**)

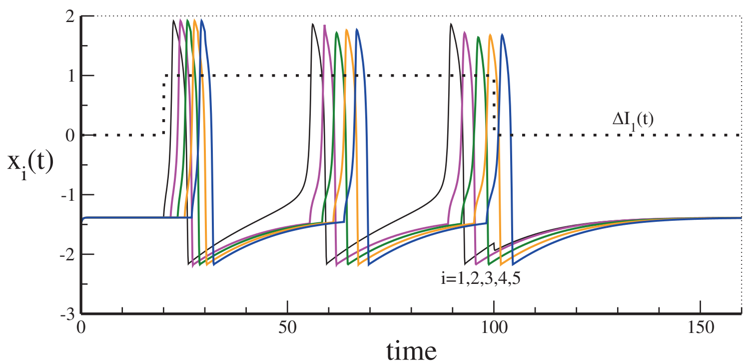

Fig. 1.10 Sample trajectories $x_i(t)$ (*lines*) for a line of coupled Terman–Wang oscillators, an example of synchronization via causal signaling. The relaxational oscillators are in excitable states, see Eq. (1.39), with $\alpha = 10$, $\beta = 0.2$, $\epsilon = 0.1$ and $I = -0.5$. For $t \in [20, 100]$ a driving current $\Delta I_1 = 1$ is added to the first oscillator. x_1 then starts to spike, driving the other oscillators one by one via a fast threshold modulation

ing rate) are important, but also the relative phasing of the individual spikes. Indeed, experimental evidence supports the notion of object definition in the visual cortex via synchronized firing. In this view neurons encoding the individual constituent parts of an object, like the mouth and the eyes of a face, fire in tact. Neurons being activated simultaneously by other objects in the visual field, like a camera, would fire independently.

The LEGION Network of Coupled Relaxation Oscillators As an example of how object definition via coupled relaxation oscillators can be achieved we consider the LEGION (local excitatory globally inhibitory oscillator network) network by Terman and Wang. Each oscillator i is defined as

$$\begin{aligned} \dot{x}_i &= f(x_i) - y_i + I_i + S_i + \rho \qquad & f(x) &= 3x - x^3 + 2 \\ \dot{y}_i &= \epsilon\big(g(x_i) - y_i\big) & g(x) &= \alpha\big(1 + \tanh(x/\beta)\big) \end{aligned} \quad . \tag{1.41}$$

There are two terms in addition to the ones necessary for the description of a single oscillator, compare Eq. (1.39):

ρ: a random-noise term and
S_i: the interneural interaction.

The interneural coupling in Eq. (1.41) occurs exclusively via the modulation of the threshold, the three terms $I_i + S_i + \rho$ constitute an effective threshold.

Interneural Interaction The interneural interaction is given for the LEGION network by

$$S_i = \sum_{l \in N(i)} T_{il}\, \Theta(x_l - x_c) - W_z \Theta(z - z_c) \ , \tag{1.42}$$

where $\Theta(z)$ is the Heaviside step function. The parameters have the following meaning:

$T_{il} > 0$: Interneural excitatory couplings.
$N(i)$: Neighborhood of neuron i.
x_c : Threshold determining the active phase.
z : Variable for the global inhibitor.
$-W_z < 0$: Coupling to the global inhibitor z.
z_c : Threshold for the global inhibitor.

Global Inhibition Global inhibition is a quite generic strategy for neural networks with selective gating capabilities. A long-range or global inhibition term assures that only one or only a few of the local computational units are active coinstantaneously. In the context of the Terman–Wang LEGION network it is assumed to have the dynamics

$$\dot{z} = (\sigma_z - z)\,\phi, \qquad \phi > 0 \ , \tag{1.43}$$

where the binary variable σ_z is determined by the following rule:

$\sigma_z = 1$ if at least one oscillator is active.
$\sigma_z = 0$ if all oscillators are silent or in the excitable state.

This rule is very non-biological, the LEGION network is just a proof of the principle for object definition via fast synchronization. When at least one oscillator is in its active phase the global inhibitor is activated, $z \to 1$, and inhibition is turned off whenever the network is completely inactive.

Simulation of the LEGION Network A simulation of a 20×20 LEGION network is presented in Fig. 1.11. We observe the following:

- The network is able to discriminate between different input objects.
- Objects are characterized by the coherent activity of the corresponding neurons, while neurons not belonging to the active object are in the excitable state.
- Individual input objects pop up randomly one after the other.

Working Principles of the LEGION Network The working principles of the LEGION network are the following:

- When the stimulus begins there will be a single oscillator k, which will jump first into the active phase, activating the global inhibitor, Eq. (1.43), via $\sigma_z \to 1$. The noise term $\sim\rho$ in Eq. (1.41) determines the first active unit randomly from the set of all units receiving an input signal $\sim I_i$, whenever all input signals have the same strength.
- The global inhibitor then suppresses the activity of all other oscillators, apart from the stimulated neighbors of k, which also jump into the active phase, having set the parameters such that

$$I + T_{ik} - W_z > 0, \qquad I: \text{ stimulus}$$

  is valid. The additional condition

$$I - W_z < 0$$

  assures, that units receiving an input, but not being topologically connected to the cluster of active units, are suppressed. No two distinct objects can then be activated coinstantaneously.
- This process continues until all oscillators representing the stimulated pattern are active. As this process is very fast, all active oscillators fire nearly simultaneously, compare also Fig. 1.10.
- When all oscillators in a pattern oscillate in phase, they also jump back to the silent state simultaneously. At that point the global inhibitor is turned off: $\sigma_z \to 0$ in Eq. (1.43) and the game starts again with a different pattern.

Discussion Even though the network nicely performs its task of object recognition via coherent oscillatory firing, there are a few aspects worth noting:

- The functioning of the network depends on the global inhibitor triggered by the specific oscillator that jumps first. This might be difficult to realize

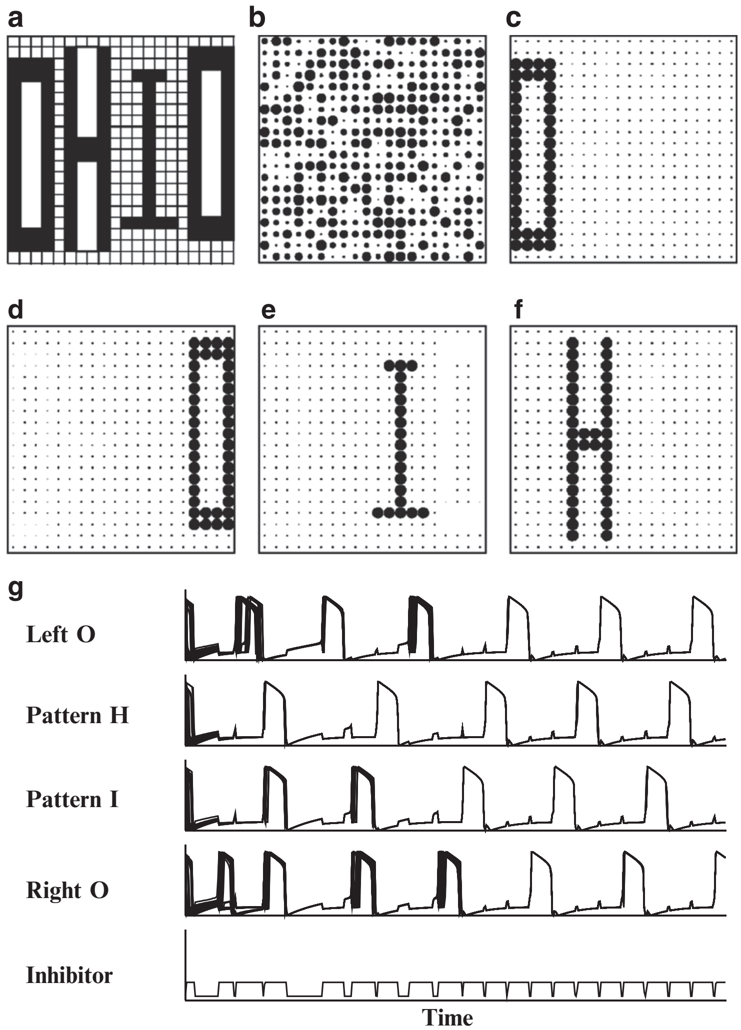

Fig. 1.11 (**a**) A pattern used to stimulate a 20 × 20 LEGION network. (**b**) Initial random activities of the relaxation oscillators. (**c**)–(**f**) Snapshots of the activities at different sequential times. (**g**) The corresponding time-dependent activities of selected oscillators and of the global inhibitor (From **? ?**)

in biological networks, like the visual cortex, which do not have well defined boundaries.
- The first active oscillator sequentially recruits all other oscillators belonging to its pattern. This happens very fast via the mechanism of rapid threshold modulation. The synchronization is therefore not a collective process in which the input data is processed in parallel; a property assumed to be important for biological networks.

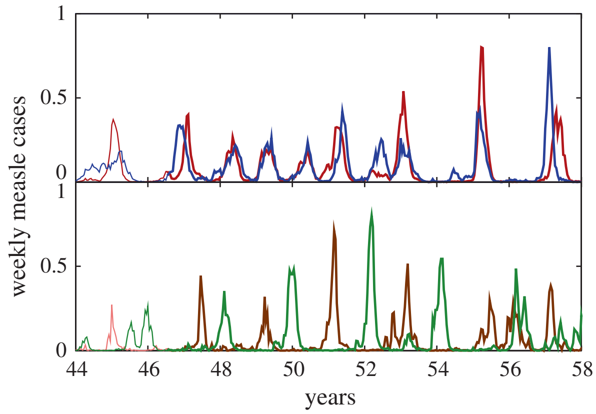

Fig. 1.12 Observation of the number of infected persons in a study on illnesses. *Top*: Weekly cases of measle cases in Birmingham (*red line*) and Newcastle (*blue line*). *Bottom*: Weekly cases of measle cases in Cambridge (*green line*) and in Norwich (*brown line*) (From **? ?**)

S	**S**	**S**	**I**	**R**	**R**	**R**	**S**	**S**	state
1	2	3	4	5	6	7	8	9	time

Fig. 1.13 Example of the course of an individual infection within the SIRS model with an infection time $\tau_I = 1$ and a recovery time $\tau_R = 3$. The number of individuals recovering at time t is just the sum of infected individuals at times $t-1$, $t-2$ and $t-3$, compare Eq. (1.44)

– The recognized pattern remains active for exactly one cycle and no longer.

We notice, however, that the design of neural networks capable of fast synchronization via a collective process remains a challenge, since collective processes have an inherent tendency towards slowness, due to the need to exchange information, e.g. via molecular fields. Without reciprocal information exchange, a true collective state, as an emergent property of the constituent dynamical units, is not possible.

1.6 Synchronization Phenomena in Epidemics

There are illnesses, like measles, that come and go recurrently. Looking at the local statistics of measle outbreaks, see Fig. 1.12, one can observe that outbreaks occur in quite regular time intervals within a given city. Interestingly though, these outbreaks can be either in phase (synchronized) or out of phase between different cities.

The oscillations in the number of infected persons are definitely not harmonic, they share many characteristics with relaxation oscillations, which typically have silent and active phases, compare Sect. 1.4.2.

The SIRS Model A standard approach to model the dynamics of infectious diseases is the SIRS model. At any time an individual can belong to one of the three classes:

S : susceptible,
I : infected,
R : recovered.

The dynamics is governed by the following rules:

(a) Susceptibles pass to the infected state, with a certain probability, after coming into contact with one infected individual.
(b) Infected individuals pass to the recovered state after a fixed period of time τ_I.
(c) Recovered individuals return to the susceptible state after a recovery time τ_R, when immunity is lost, and the S $\to$ I $\to$ R $\to$ S cycle is complete.

When $\tau_R \to \infty$ (lifelong immunity) the model reduces to the SIR-model.

The Discrete Time Model We consider a discrete time SIRS model with $t = 1, 2, 3, \ldots$ and $\tau_I = 1$: The infected phase is normally short and we can use it to set the unit of time. The recovery time τ_R is then a multiple of $\tau_I = 1$.
We define with

x_t the fraction of infected individuals at time t,
s_t the percentage of susceptible individuals at time t,

which obey

$$s_t = 1 - x_t - \sum_{k=1}^{\tau_R} x_{t-k} = 1 - \sum_{k=0}^{\tau_R} x_{t-k} \ , \tag{1.44}$$

as the fraction of susceptible individuals is just 1 minus the number of infected individuals minus the number of individuals in the recovery state, compare Fig. 1.13.

The Recursion Relation We denote with a the rate of transmitting an infection when there is a contact between an infected individual and a susceptible individual:

$$x_{t+1} = a x_t s_t = a x_t \left(1 - \sum_{k=0}^{\tau_R} x_{t-k} \right) \ . \tag{1.45}$$

Relation to the Logistic Map For $\tau_R = 0$ the discrete time SIRS model (1.45) reduces to the logistic map

$$x_{t+1} = a x_t \left(1 - x_t\right) \ ,$$

which we studied in Chap. **??**. For $a < 1$ it has only the trivial fixpoint $x_t \equiv 0$, the illness dies out. The non-trivial steady state is

$$x^{(1)} = 1 - \frac{1}{a}, \qquad \text{for} \quad 1 < a < 3 \ .$$

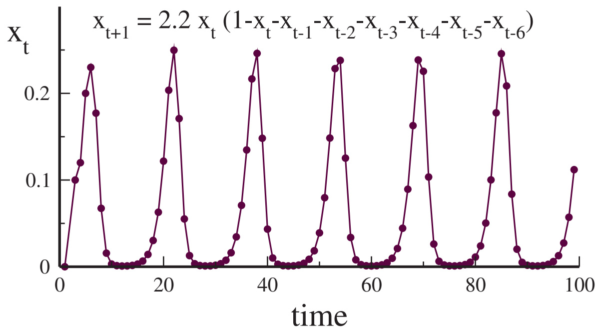

Fig. 1.14 Example of a solution to the SIRS model, Eq. (1.45), for $\tau_R = 6$. The number of infected individuals might drop to very low values during the silent phase in between two outbreaks as most of the population is first infected and then immunized during an outbreak

For $a = 3$ there is a Hopf bifurcation and for $a > 3$ the system oscillates with a period of 2. Equation (1.45) has a similar behavior, but the resulting oscillations may depend on the initial condition and for $\tau_R \gg \tau_I \equiv 1$ show features characteristic of relaxation oscillators, see Fig. 1.14.

Two Coupled Epidemic Centers We consider now two epidemic centers with variables

$$s_t^{(1,2)}, \qquad x_t^{(1,2)},$$

denoting the fraction of susceptible/infected individuals in the respective cities. Different dynamical couplings are conceivable, via exchange or visits of susceptible or infected individuals. We consider with

$$x_{t+1}^{(1)} = a\left(x_t^{(1)} + e\,x_t^{(2)}\right)s_t^{(1)}, \qquad x_{t+1}^{(2)} = a\left(x_t^{(2)} + e\,x_t^{(1)}\right)s_t^{(2)} \tag{1.46}$$

the visit of a small fraction e of infected individuals to the other center. Equation (1.46) determines the time evolution of the epidemics together with Eq. (1.44), generalized to both centers. For $e = 1$ there is no distinction between the two centers anymore and their dynamics can be merged via $x_t = x_t^{(1)} + x_t^{(2)}$ and $s_t = s_t^{(1)} + s_t^{(2)}$ to the one of a single center.

In Phase Versus Out of Phase Synchronization We have seen in Sect. 1.2 that a strong coupling of relaxation oscillators during their active phase leads in a quite natural way to a fast synchronization. Here the active phase corresponds to an outbreak of the illness and Eq. (1.46) indeed implements a coupling equivalent to the fast threshold modulation discussed in Sect. 1.4.2, since the coupling is proportional to the fraction of infected individuals.

In Fig. **??** we present the results from a numerical simulation of the coupled model, illustrating the typical behavior. We see that the outbreaks of epidemics in the SIRS model indeed occur in phase for a moderate to large coupling constant e. For very small coupling e between the two centers of epidemics on the other hand, the synchronization becomes antiphase, as is sometimes observed in reality, see Fig. 1.12.

Time Scale Separation The reason for the occurrence of out of phase synchronization is the emergence of two separate time scales in the limit $t_R \gg 1$ and $e \ll 1$. A small seed $\sim e a x^{(1)} s^{(2)}$ of infections in the second city needs substantial time to induce a full-scale outbreak, even via exponential growth, when e is too small. But in order to remain in phase with the current outbreak in the first city the outbreak occurring in the second city may not lag too far behind. When the dynamics is symmetric under exchange $1 \leftrightarrow 2$ the system then settles in antiphase cycles.